



www.maajournal.com

Mediterranean Archaeology and Archaeometry
Vol. 22, No 3, (2022), pp. 31-44
Open Access. Online & Print.



DOI: 10.5281/zenodo.7072720

LEAD STANNATE AS COMPONENT OF ANTIQUE YELLOW GLASSY TESSERAE FROM SICILIAN MOSAICS

Marcella Di Bella^{1,2}, Giuseppe Sabatino^{2*}, Maria Amalia Mastelloni³,
Francesco Italiano¹, Maurizio Triscari², Giuseppe Marcianò²,
Antonio Francesco Mottese² and Alessandro Tripodo²

¹*Istituto Nazionale di Geofisica e Vulcanologia (INGV), Sezione di Palermo, Sede Operativa di Milazzo,
Via dei Mille 46, 98057 Milazzo (ME), Italy*

²*Dipartimento di Scienze Matematiche e Informatiche, Scienze Fisiche e Scienze della Terra (MIFT),
Università di Messina, Viale Stagno d'Alcontres 31, 98166 Messina, Italy*

³*Polo Regionale delle Isole Eolie, Parco, Museo Archeologico "L. Bernabò Brea", Lipari, Italy*

Received: 05/08/2022

Accepted: 15/09/2022

*Corresponding author: Sabatino Giuseppe (gsabatino@unime.it)

ABSTRACT

New investigations carried out on lead stannate (Pb_2SnO_4) and lead antimonate ($\text{Pb}_2\text{Sb}_2\text{O}_7$) in yellow mosaic glassy tesserae from archaeological sites of Sicily (Taormina; Lipari, Tusa and Piazza Armerina), dated early than the 4th century AD, allow to confirm the presence of lead stannate in ancient glass dated before the 4th century. The two compounds have been used either as glass opacifiers and colorants. The different refractive index between fine crystals of these compounds and the amorphous glassy matrix, in which they are immersed, prevent the complete light transmittance, giving the typical opaque appearance to the glass. While lead antimonate was used to produce opaque yellow glass from the beginning of glass production up to the Roman period, it was replaced by lead stannate from about the 4th century AD up to the end of the Roman period. Although until today only Lahil et al. (2011) reported the presence of lead stannate in the glass tesserae dated before the 4th century AD, our new results confirm its presence in the investigated yellow tesserae from several mosaics of Sicily dated early than the 4th century AD.

KEYWORDS: Roman age, mosaic tesserae, yellow glass, lead stannate, SEM-EDS, XRD, Sicily

1. INTRODUCTION

Pb antimonate compounds were used to produce opaque glass from the beginning of glass production up to the Roman period (3–4th AD). According to some authors it was initially used as opacifying agent in Egyptian yellow glasses began about 3500 B.P. (Wainwright et al., 1986). About 1500 B.C. the Egyptian dynasty used lead and antimony compounds to give yellow glass objects. Lead antimonate was also known in the Mesopotamia, Babylonian and Assyrian cultures (Hedges et al., 1976). Turner and Rooks (1979) have identified lead tin antimonate in mosaic glass tesserae from a Byzantine church in Novgorod (Russia). Another example of medieval usage of mixed lead stannate and antimonate has been reported for an Islamic enameled bottle from Syria, dated to 14th century.

These Pb antimonate compounds have been used both for the decoration of ceramics and as pigments. In Italy, the first objects containing these opacifiers range from 4th to 3rd centuries BC. Its presence, within the glass matrix, led to a color ranging from opaque yellow to green yellow. As opacifying agent it is identified in form of lead antimonate ($\text{Pb}_2\text{Sb}_2\text{O}_7$) as evidenced in several studies conducted by means of EMPA, XRF and XRPD analyses and more recently by Raman spectroscopy (e.g. Mass et al., 1997; Shortland, 2002; Kaplan et al., 2017; Raneri et al., 2018; Gelzo et al., 2021; Giustetto et al., 2018; De Francesco et al., 2019; Belfiore et al., 2021).

From a chemical perspective, it is a lead antimonate ($\text{Pb}_2\text{Sb}_2\text{O}_7$), having a cubic pyrochlore structure, although different types of cubic pyrochlore are known as synthetic pigments (Cascales et al., 1985, 1986; Rosi et al., 2009). An analogue of lead antimonate is the natural mineral bindheimite (Dik et al. 2005; Rosi et al., 2009), mainly occurring in the oxidized portions of antimony-bearing lead deposits as a frequent oxidation product of Pb-Sb-sulphosalts (Hradil et al., 2007), however it has never been employed as pigment (Wainwright et al., 1986).

This mineral can be found as thin weathering crusts in ore outcrops in some region of Italy, Spain, Britain and Greece (Dana, 1951; Dessau, 1951; Clayton, 1990). The only substantial deposit of bindheimite within the Roman Empire occurs at Djebel Slata, in Tunisia. Although, this region of North Africa was crossed by many Roman trade routes, there is no reference to either use or trade of this mineral in the classical literature, and it is very unlikely that the Romans sought out this rare material as pigment (Charlesworth, 1924).

This is supported by an examination of the Roman palette for wall paintings, which reveals that they used iron ochres, orpiment, and realgar as yellow pigments (Augusti, 1967). $\text{Pb}_2\text{Sb}_2\text{O}_7$ is a brighter and more robust

pigment than the iron- or arsenic-based yellows, and so if this pigment were mined from North African bindheimite use in Roman wall painting would be expected (Mass et al., 1998). At the end of the Roman Empire, however, the use of lead antimonate as opacifying agent for glass seems to have drastically decreased (Turner et al., 1959, Tite et al., 2008). We must wait for the beginning of the 15th century to find a new intensive use of this opacifying/colouring agent, especially in glass, ceramics or as a pigment in paintings (Wainwright et al., 1986, Hedges et al., 1976). This type of color was called “Giallo Napoli” or “Giallo Antico”. The time of reintroduction of “Giallo Napoli” in the Western world, particularly in Italy, is not clearly assessed and could have happened in the second half of the 15th century A.D. (Dik et al., 2005).

The use of Sn antimonate compounds for the production of yellow ceramic pigments is firstly mentioned by Vannoccio Biringuccio (1540) in his book “De la Pirotechnia” (cf., the second volume, *Del antimoinio et de sua miniera*, pag. 27), and then by Cipriano Piccolpasso (1548) in the treatise “Li tre libri dell’arte del vasaio” where 15 different recipes for the production of yellow pigment using both lead and antimony are reported. However, “Giallo Napoli” was certainly used by the Romans in around the first and second centuries BC, to obtain yellow glasses (Mass et al., 1998).

Afterwards, according to some authors (Turner and Rooksby, 1959; Bimson and Werner, 1969), the pigment was progressively substituted by Pb-Sn compounds. Possibly due to the downfall of the Western Roman Empire (476 AD) and to the change of commercial routes, the recipe for production of this pigment in the Western World has been lost (Dik et al., 2005; Seccaroni, 2006). In fact, during the Middle Ages, yellow glazes and glasses were apparently obtained by recycling Roman glasses (Seccaroni, 2006). On the contrary, Pb-Sb compounds continued to be produced and employed only in the Islamic (Seccaroni, 2006) and Byzantine worlds, as recently observed in late Byzantine glazed pottery from Turkey and the Former Yugoslav Republic of Macedonia (Tanevska et al., 2009; Kirmizi et al., 2014). Only Lahil et al. (2011) reported the presence of lead stannate in glass tesserae dated before the 4th century AD.

With the aim to broaden the knowledge about the use of lead stannate as colouring and opacifying agent before 4th century A.D., we have analyzed its presence in mosaic glassy tesserae from Taormina (2nd cent. B.C.), Lipari, Tusa and Piazza Armerina (3–4th cent. AD) archaeological sites (Fig. 1). The used analytical approach includes Scanning Electron Microscopy (SEM-EDS), X-ray Diffraction and Ultraviolet-visible-near infrared spectroscopy (UV VIS-NIR).



Figure 1. Mosaics from which come the studied yellow tesserae

2. MATERIALS AND METHODS

A total of 19 yellow opaque glass tesserae (Fig. 2) were collected for this study. The samples come from mosaics of the following archaeological sites:

1) Taormina n. 1 (TAO) – tesserae from the in situ preserved floor, via Circonvallazione n.° 3 "La Campanella" Villa - the yellow glassy tesserae are inserted in the frame of a white-tesserae floor, it is dated to the 2nd century BC (Boeselager, 1983; M.A. Mastelloni, 2004, 2005).

2) Tusa n. 1 (GT2) – tesserae in floor-mosaics discovered in 1912 at Lancinè district, over 10 km southwest from the archaeological site of the Halesa city (currently exhibited in the Tusa Antiquarium). These materials have been dated to the 3rd century AD, for both stylistic and analogies with mosaics from Bagnoli-S. Gregorio (Capo d' Orlando). Three rooms have been found, the third of which is larger than the others, it appears to be a triclinium, decorated with a triple pattern lines with double dark tesserae forming a broken meander and, in the intermediate spaces, swastikas. These decorations define octagonal spaces in which they are found with plant and animal motifs (Boeselager, 1983; Mastelloni, 2001; 2004).

3) Lipari n. 1 (GL10) – tesserae from floor recovered in 1912, between via Umberto I and Piazza Monfalcone (Renda house at the foot of the fortress) and currently exhibited at the Regional Museum of Messina (Mastelloni et al., 2011). The dimensions of the panel, almost square, are approximately 122 x 115 cm; the decoration consists of the busts of the four seasons on

the diagonals, with a center figure representing a female riding on a large bull. For comparison with Tusa and Capo d' Orlando (Bagnoli - S. Gregorio) mosaics, they have been dated to 3rd century AD (Mastelloni, 2004).

4) Piazza Armerina (EN) n. 16 (PAG 5-1, PAG 5-2, PAG 5-3, PAG 5-4, PAG 5-6, PAG 5-7, PAG 5-8, PAG 5-10, PAG 8-1, PAG 8-2, PAG 8-3, PAG 8-4, PAG 8-5, PAG 8-6, PAG 9-7, PAM 1) – tesserae from in situ floor, Villa Romana del Casale, with over 3,500 m² of mosaics extent (Gentili, 1954). It is among the most extraordinary mosaic decorations - for the complexity of the iconographic apparatus - that has no comparison even in the mosaics of the Romans Tunisian villas. From the African area were probably the masters, which between the 3rd and 4th cent. AD, provided the to the Empire the schools of mosaic decorations (Wilson, 1982). Thus, based on stratigraphy, historical data and literary sources, the villa was dated to the 340 AD. The villa probably belonged to a personality from the hierarchy of the Roman Empire, some suggest who is probably a senator and patrician also awarded by the consulate, according to others he is the M. Valerio Massimino Emperor, called Herculeos Victor.

All the 19 samples were chemically analyzed by Scanning Electron Microscopy Analysis (SEM-EDS) in order to identify textures and inclusions, and by XRD to define the mineralogical composition. Ten samples (PAG 5-1, PAG 5-2, PAG 5-3, PAG 5-4, PAG 5-6, PAG 5-7, PAG 5-8, PAG 5-10, PAG 8-1, PAG 8-2, PAG 8-3, PAG 8-4, PAG 8-5, PAG 8-6, PAG 9-7, PAM

1, GT2, GL10, TAO) were analyzed by Ultraviolet-visible- near infrared spectroscopy (Uv-Vis-NIR) to determine mineralogical composition and to compare the results with XRD data. Lastly, 17 samples (PAG 5-2, PAG 5-3, PAG 5-4, PAG 5-6, PAG 5-7, PAG 5-8, PAG 5-10, PAG 8-1, PAG 8-2, PAG 8-3, PAG 8-4, PAG

8-5, PAG 8-6, PAG 9-7, PAM 1, GT2, GL10, TAO) were analyzed by EMPA (electron micro-probe analyzer) to identify bulk chemical composition (PAG 5-2, PAG 5-3, PAG 5-4, PAG 5-6, PAG 5-7, PAG 5-8, PAG 5-10, PAG 8-1, PAG 8-2, PAG 8-3, PAG 8-4, PAG 8-5, PAG 8-6, PAG 9-7, PAM 1, GT2, GL10, TAO).

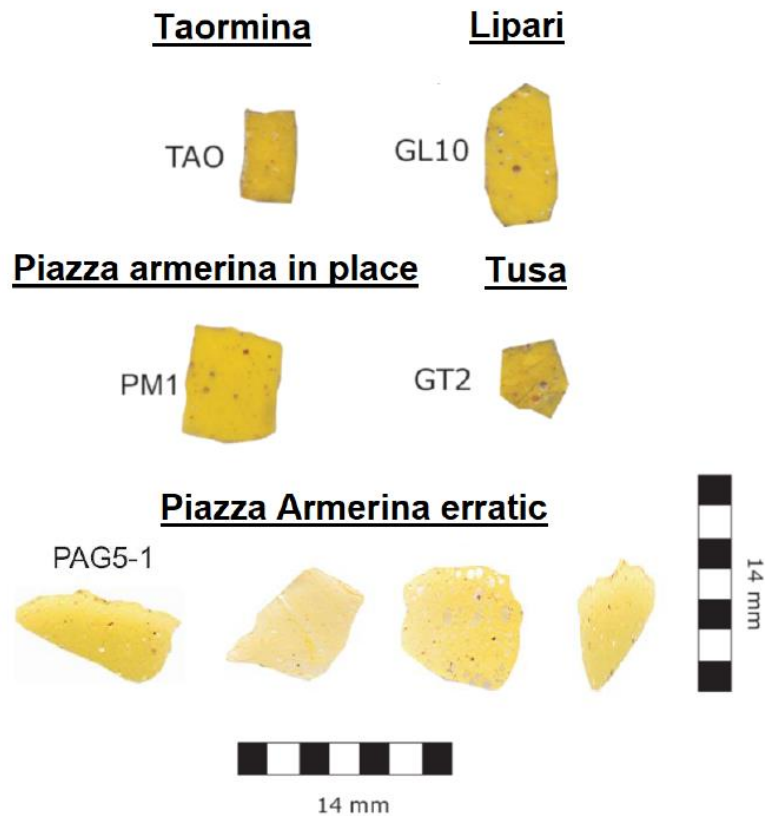


Figure 2. The studied yellow tesserae.

2.1. Scanning Electron Microscopy Analysis (SEM-EDS)

The textural investigations of the 5 selected samples were performed at the SEM-EDS laboratory of the Earth Science Department of Messina University, using an ESEM-FEI Inspect-S, Electron Microscope coupled with Oxford INCA PentaFETx3 EDX spectrometer, is a Si(Li) detector, nitrogen cooled, equipped with an ultra thin window ATW2. Its resolution is of 137 eV at 5.9 keV (Mn K α 1). The spectral data were acquired at working distance of 10 mm with an acceleration voltage of 20 kV, counting times of 60 seconds, counts/second approximately 3000 cps. The results were processed by INCA software Energy. This software uses the XPP matrix correction scheme developed by Pouchou and Pichoir (1984; 1985). This type of correction matrix has a better performance compared with ZAF and ϕ - ρ -z widespread used

2.2. X-ray diffraction (XRD)

The X-ray diffraction experiments were performed at the Diffractometric Laboratory of Messina University, with a BRUKER D8 ADVANCE diffractometer with Cu K α radiation on a Bragg-Brentano theta-theta goniometer, equipped with a SiLi solid-state detector, Sol-X. Acquisition conditions are 40 KV and 40 mA. Scans are obtained typically from 2 to 80 degrees 2 theta, with step size of 0.02 degrees 2theta, with a count time of 1 second. Raw diffraction scans are stripped of K α 2 component, background corrected with a digital filter (or Fourier filter). Observed peak positions are matched against the ICDD-JCPDS database

2.3. Ultraviolet-Visible-near-IR Spectroscopy UV - Vis - NIR

The absorption spectra were a Perkin Elmer L20 spectrophotometer UV-Vis (range 180 - 1100 nm). Current-voltage curves were recorded by a digital

Keithley 236 multimeter connected to a PC and controlled by a homemade program. Simulated sunlight irradiation was provided by a LOT-Oriel solar simulator (Model LS0100-1000, 300 W Xe Arc lamp powered by LSN251 power supply equipped with AM 1.5 filter, 100 mW/cm²). Incident irradiance was measured with a Si-based pyranometer. Incident photon-to-current conversion efficiency (IPCE) and relative photoaction spectra of sealed DSSCs were measured by a IPCE station. The IPCE station was composed by a 150 Xenon Light Source (model ASB-XE, Spectral Products), a Monochromator (model CM110, Spectral Products) equipped with a slit set, a Si calibrated detector (model 818-UV, Newport), a Picoamperometer (model 6487, Keithley) and a IPCE Solarena Software. The photoanodes thickness was measured by using a DektakXT profilometer (Bruker) equipped with a diamond-tipped stylus (radius of 2 μ m) and selecting a vertical scan range of 65 μ m with 8.0 nm resolution, a programmed scan length of 6000 μ m, and a stylus force of 1 mg. Each measure was verified by acquiring different runs with different start positions, by rotating or translating the sample.

3. RESULTS

3.1. Major elements and glass classification

Results of EMPA analyses carried out on 16 yellow tesserae (PAG 5-1, PAG 5-2, PAG 5-3, PAG 5-8, PAG 5-

10, PAG 8-1, PAG 8-2, PAG 8-3, PAG 8-4, PAG 8-5, PAG 8-6, PAG 9-7, PAM, TAO, GL10, GT21) are already published and reported in Sabatino (PhD thesis, 2007) and Di Bella et al. (2013). Major components of the glass matrix vary in the following ranges: SiO₂ from 62 % to 72 %, Na₂O from 16 % to 19 %, CaO from 5 % to 9 % and Al₂O₃ from 1.9 % to 4.4 %.

According to Croveri et al. (2010) and Di Bella et al. (2013), the analysed glasses can be classified as natron-based, as displayed on the K₂O vs. MgO classification diagram shown in Fig. 3. This type of raw glass is a peculiar feature of Roman and Byzantine glasses produced with siliceous-calcareous sands over the Western Mediterranean area, (e.g., Turner, 1956; Sayre and Smith, 1974; Henderson, 1985; Verità, 1995; Freestone et al., 2002a, b; Sabatino, 2007; Arletti, 2005; Arletti et al., 2005, 2010) and characterized by low MgO and K₂O contents (less than 1.1 %) and high Na₂O content usually ranging from 14 % to 19 %. In Europe, natron-like glass was widely used in glass production from the sixth and seventh centuries BC up to the end of the first millennium AD, when it was replaced by plant ash (Lilyquist and Brill, 1995).

Bulk elemental analyses show that all samples contain very low antimony amounts (0.01 < Sb₂O₃ < 0.8 wt %), impeding the measurement of the antimony oxidation state and to use it as an indicator of the opacification process (Lahil et al., 2010).

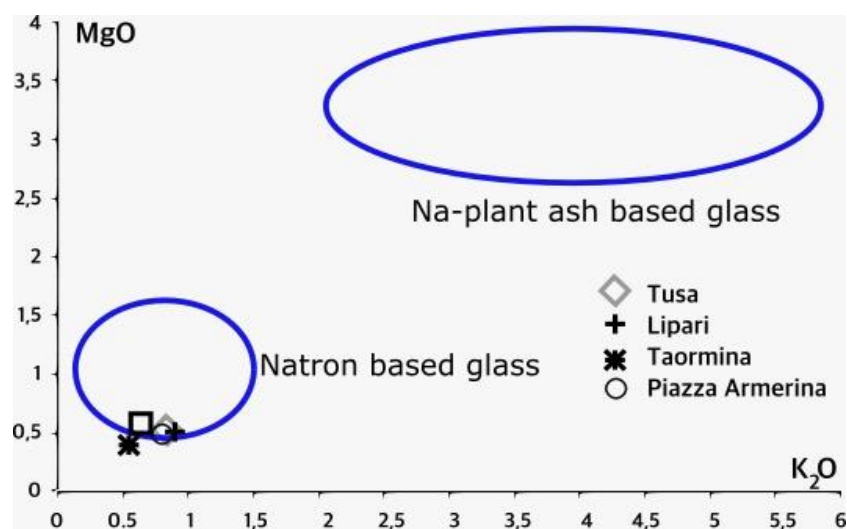


Figure 3. K₂O vs MgO classification diagram for the studied yellow glassy tesserae

3.2. Full characterization of Pb-stannate and Pb-antimoniate opacifying/colouring agents

The most common textures observed in the yellow tesserae are displayed in Fig. 4. Typically, the yellow tesserae show laminar textures with alternated layers, due to the stratification of fine particles (< 2 micron), indistinguishable through optical microscopy. Those layers are variably distributed and organized to produce from sub-parallel (Fig. 4 a-b-c-d) to convoluted

chaotic textures (Fig 4 a-e-f). Furthermore, all the analyzed yellow tiles show abundant, variably deformed bubbles, which are statically grown on the laminar structures (Fig. 4). In the sub-parallel textures the bubbles display more or less circular shape, while in the chaotic texture they are more elongated showing ellipsoidal shapes. These bubbles are particularly abundant in most of the analyzed samples, in which

both types spherical and elongated have been observed.

Moreover, SEM-EDS analyses (Tab. 1) and observation (Fig. 4) of glass-evidenced the presence of dark

areas characterized by values of SiO₂, Na₂O and CaO higher than the surrounding light glassy matrix, which show instead higher PbO values and lower SiO₂.

Table 1. Representative SEM-EDS data related to dark and light areas analyzed for the studied yellow tesserae.

Oxides %	Dark areas			Light areas		
Na ₂ O	10.7	12.3	14.16	8.7	9.12	9.8
Al ₂ O ₃	2.5	3	2.39	7.3	3.97	1.6
SiO ₂	75.5	71.7	72.17	43.5	55.46	58.1
Cl	-	0.5	0.4	-	0.23	0.4
K ₂ O	0.7	1.1	1.07	-	0.95	0.9
CaO	6	7.2	7.67	4.5	3.82	5.2
MnO	-	-	0.66	-	0.49	0.4
Fe ₂ O ₃	-	1	0.57	2.4	1.21	0.7
PbO	4.1	2.5	1.2	33	24.41	22.2
Total	99.5	99.3	100.29	99.4	99.66	99.3

SEM-EDS analyses allowed to characterize the opacifiers from the morphological and chemical point of view. Results show the presence of different sized grains (from 50-80 to 20 microns) engrouped to form aggregates homogeneously distributed (Fig. 4 and 5). They appear bright to SEM-BSE observations, probably due to the high content in Pb and Sn. At high magnifications the opacifier particles form, according to Lahil et al 2011, aggregates of various shapes and, as mentioned before, various sizes. All samples show great clusters of lead antimonate and lead stannate dispersed in the glassy matrix, typically characterized by chemical disequilibrium structures with resorbed rims, due to partial fusion (Fig. 5b-c). On the chemical point of view the opacifier particles are composed of Pb, Sb and Sn (Tab. 2).

They are abundantly noticeable in the sample PAG (Fig. 5d) where they have shapes ranging from the

pseudo circular to elongated ellipsoids. In secondary electron SEM images they have a predominantly black colour and, as shown by Tab. 3, some EDX investigations have been carried out to detect their chemical composition. The areas in which the bubbles prevail, compared to the glass mass in which they are included, have a composition marked by SiO₂, Na₂O, CaO, Al₂O₃ and Fe₂O₃. Conversely, the areas around the bubbles, where the laminar background mass of the glass is present, exhibit higher PbO and lower SiO₂ content. In some samples, however, it has been possible to detect perfectly euhedral particles (Fig. 5c), present almost exclusively in the samples of Piazza Armerina, and in other cases an acicular morphology (Fig. 5d) probably caused by a rapid cooling of the sample.

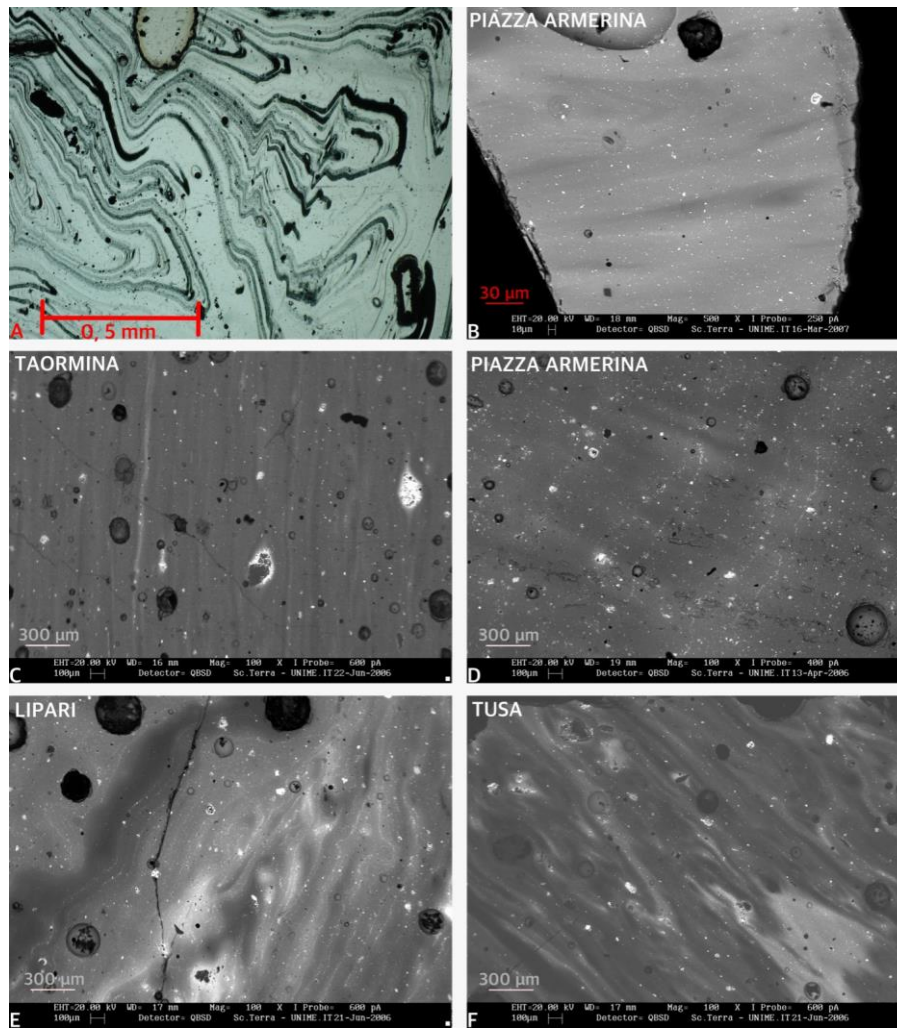


Figure 4. Microphotography (a) and SEM-EDS images (b-f) of lead antimonate and stannate in layered texture due to stratification of fine particles. a,d,f) convolute-chaotic texture; b,c,e) subparallel layers. All the images exhibit the presence of light and dark areas characterized by different silica and lead content

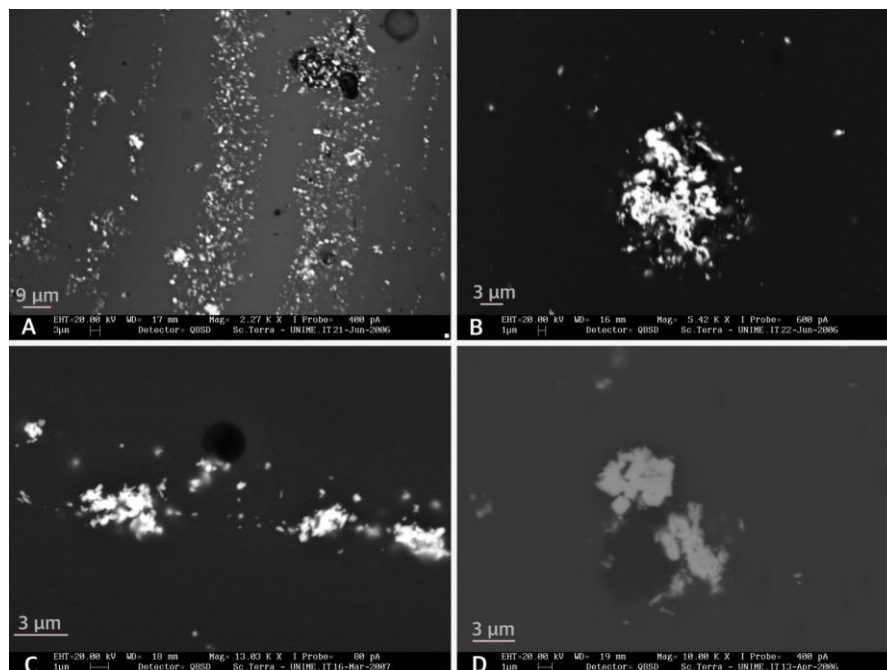


Figure 5. SEM-EDS images of lead antimonate and stannate particles

Table 2. SEM-EDS data of Pb-antimonate, stannate and Pb-Sn-Sb mixed compounds analysed for the studied yellow tesserae

Oxides %	Pb-antimonate			Pb- stannate			Pb-Sn-Sb mixed compounds		
Na ₂ O	3.80	8.26	2.00	-	3.90	0.80	1.30	1.41	1.90
Al ₂ O ₃	-	2.65	-	-	2.20	-	-	-	-
SiO ₂	13.70	36.10	14.20	6.25	7.80	5.90	4.50	6.71	5.00
CaO	-	2.57	-	-	-	-	1.80	2.70	-
Fe ₂ O ₃	2.80	5.08	2.60	1.33	-	0.50	1.50	-	-
SnO ₂	-	-	-	27.06	36.70	28.60	16.60	12.45	18.90
Sb ₂ O ₃	22.54	15.68	24.50	-	-	-	26.40	25.34	19.10
PbO	56.50	30.10	57.20	64.36	50.20	63.90	47.50	50.57	54.30
Total	99.34	100.44	100.50	99.00	100.80	99.70	99.60	99.18	99.20

The nature of the yellow colorant opacifier was identified on the basis of all analysis method, chemical, diffractometric and UV-Vis-NIR data. Yellow tiles are characterized by relatively high amounts of Pb and remarkable amounts of Sb. XRD patterns (Fig. 6) show the typical high background due to the glass matrix, but also the peaks of a crystalline phase lead antimonate, identified as bindheimite Pb₂Sb₂O₇ (PDF number 042-1355). The low amount of lead stannate does not allow its identification on the XRPD pattern. The UV-VIS-NIR pattern (Fig. 7) show similar characteristics among them:

1) maximum absorption between 410-420 nm, very broadband starting absorption at about 460;

2) a shoulder more or less marked at about 480 nm;

3) This main absorption band is observed with the same characteristics in all the yellow glass investigated, the only discernible difference is that the absorptions are less marked in the GT2, GL10, TAO samples, (Fig. 7a)

4) Between the 610 – 700 nm the samples PAM1 show a plateau, due to an absorption decrease

5) Some erratic tiles from Piazza Armerina (PAG series), near 610 nm show a minimum absorption phase with a substantial recovery after 625-630 nm (Fig. 7b)

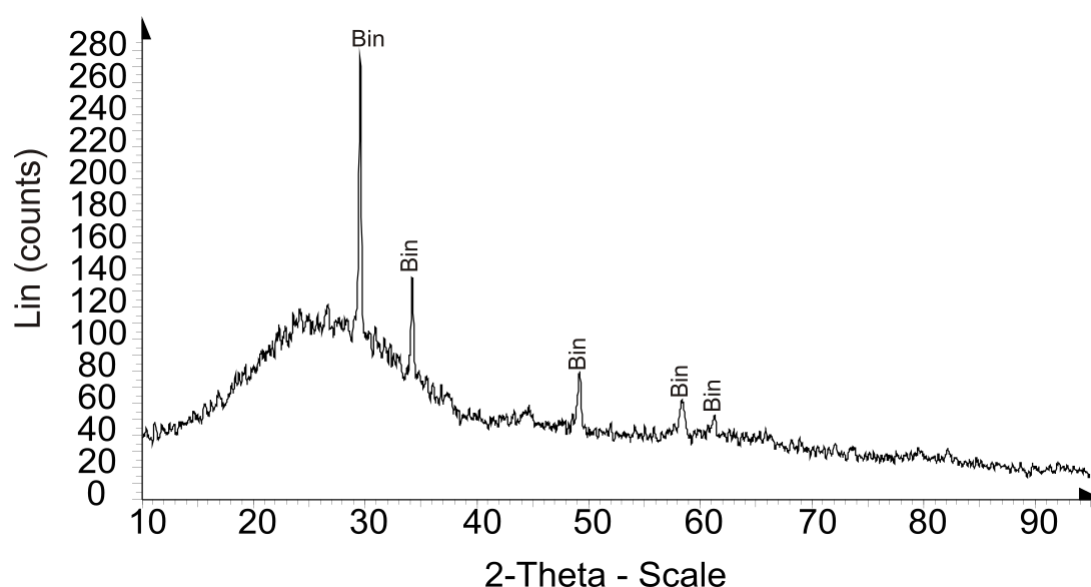


Figure 6. Representative XRPD pattern of bindheimite identified in the studied yellow glass

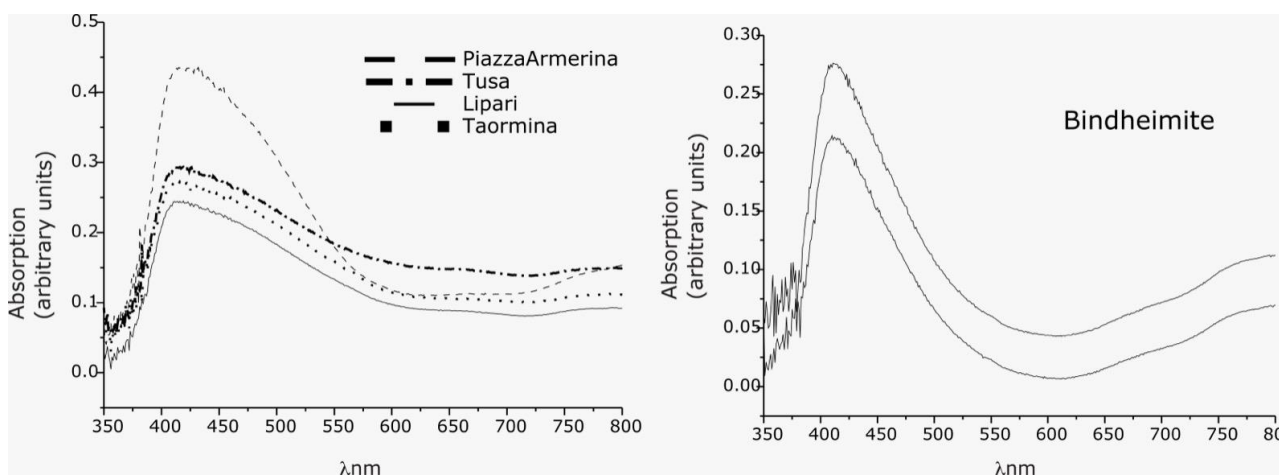


Figure 7. Representative UV-VIS spectra of yellow studied glass and of bindheimite

4. DISCUSSION

The most common laminar textures with alternated layers observed in the yellow tiles, displayed in Fig. 7 a and b, is due to the stratification of fine particles (< 2 micron) in layers variably distributed and organized to produce from sub-parallel (Fig. 4 a-b-c-d) to convoluted chaotic (Fig. 4 a-e-f) textures. This last feature can be interpreted as a tentative of homogenizing the melt glass during the mechanically addition of the colouring/opacifying agents (Arletti, 2006 a, b) as also supported by the presence of abundant, variably deformed bubbles, which are statically grown on the laminar structures (Fig. 4).

The nature of the yellow colorant opacifier was constrained by chemical and diffractometric data. Yellow tiles are characterized by relatively high amounts of Pb and remarkable amounts of Sb (Tab. 2) and by the peaks of a crystalline phase lead antimoniate, identified as bindheimite $Pb_2Sb_2O_7$ on the XRD patterns (Fig. 6 b). Bindheimite is one of the most used yellow colouring agents in the technological history of glass making (Shortland 2002, 2005, 2006; Sabatino et al., 2003; Sabatino, 2007; Galli et al., 2004; Spadaro et al. 2007), and has been already found by Croveri et al (2010) in PA tesserae and by Triscari et al. (2007) in glass tesserae from a number of Sicilian archaeological sites. In our samples, bindheimite is present in both resorbed (prevalent) and euhedral (rare) crystals (Fig. 7 c and d). The presence of the two different

bindheimite morphologies is linked to the glass manufacturing process and to the modes of bindheimite addition. Starting from mixture of several oxides of the elements Pb and Sb, at temperature of around 600 °C, Pb antimoniate is obtained. Subsequently, the Pb antimoniate was added to molten glass and mechanically homogenized. This addition caused a chemical-physical disequilibrium of the phase which assumes the appearance of resorbed crystal (Fig. 7 e; Sabatino, 2007; Triscari et al. 2007). Whereas, the euhedral morphologies are considered as secondary, they probably grew in the glass as it cooled as said Shortland (2002) or are due to re-crystallization from re-heating during the manufacturing production of tesserae as proposed in this work.

Detailed micro-chemical SEM-EDS analyses on lead antimoniate revealed the presence of impurities represented by Fe_2O_3 (0.5-2 %) and of Sn compound. Those features was found by Lahlil et al. (2011) in a study performed on yellow tesserae from Roman mosaic (2nd c. BC-5th c. AD). The authors said that the Fe_2O_3 was probably introduced with the opacifier raw material and highlighted the presence of Sn bearing zone inherited the Pb antimoniate crystals. Moreover, they evidenced that in the Egyptian glass, Zn and Fe_2O_3 impurities are contained in the Pb-antimoniate crystals, whereas the Roman glass contains Sn and Fe_2O_3 . This latter feature is perfectly in agreement with the results obtained for the PA glasses, as shown in the Fe_2O_3 vs SnO_2 binary plot and in the $PbO-SnO_2-Sb_2O_3$ ternary diagram reported in Fig. 8 a and b.

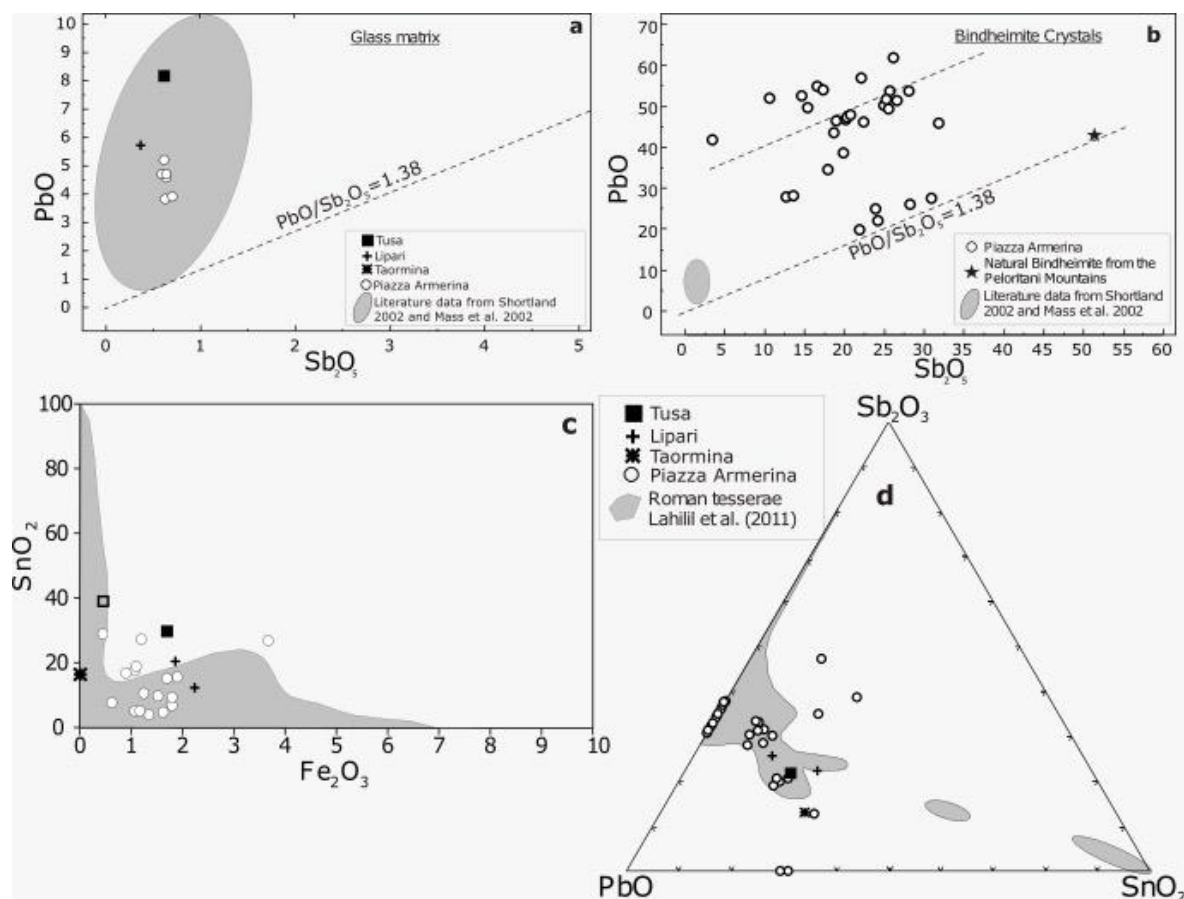


Figure 8. Sb_2O_5 vs PbO binary diagrams that evidenced in *a* the lead excess with values content of the groundmass fall inside the shaded area which is obtained from the literature data (Shortland, 2002; Mass *et al.*, 2002), in *b* the great lead excess of Pb antimonate crystals. In *c* and *d*, Fe_2O_3 vs SnO_2 binary and PbO - SnO_2 - Sb_2O_3 ternary diagrams on which the yellow tesserae from Tusa, Lipari, Taormina and Piazza Armerina (Sabatino, 2007) fall within and near the grey area traced by Lahilil *et al.* (2011) for their studied samples.

However, as regard the presence of Sn-bearing bindheimite, we found it in other studies carried out on similar yellow tiles from Sicilian and Campanian mosaics from the Messina province (e.g. Tusa, Lipari and Taormina) and the Pompei archaeological site, respectively (Sabatino, 2007; 1st c. BC to the 4th-5th c. AD). As reported in literature (see for a review Arletti *et al.*, 2011 and references), while antimony-based opacifiers (specifically, lead antimonates for yellow) had been used since the earliest time of glass production – in the Near East and Egypt around 1500 BC, and through Roman times – during the fourth century AD tin-based opacifiers started systematically to replace the antimony-based ones (Tite *et al.*, 2007), spreading from the eastern Mediterranean to northern Europe.

The stoichiometric Pb and Sb oxides proportions in $Pb_2Sb_2O_7$ are: 58% and 42%, respectively, corresponding to a PbO/Sb_2O_5 ratio of 1.38. As evident in Figure 8, this ratio is not respected in the chemical composition of the yellow tiles, always containing lead in excess. In particular, the lead content of the groundmass (Fig. 8 a) falls inside the field of literature data (shaded area) (Shortland, 2002; Mass *et al.*, 2002). The

Pb antimonate crystals, analyzed notwithstanding their small size, show a large lead excess with the data falling parallel to the theoretical PbO/Sb_2O_5 straight line (Fig. 8 b). This result is linked to crystal dimension, because analyses performed on large aggregates of bindheimite, plot very close to the PbO/Sb_2O_5 straight line. In general, the EDS and morphological studies of these tiles highlighted compositional features, which include the presence of: 1) two glass types in the groundmass of several tiles, one Pb -rich and another one Pb -free (both Sb -free); 2) Sb only inside the opacifier crystals, which are immersed in the Pb -rich glass matrix; 3) opacifier crystals with both main corroded and subordinate euhedral habitus. To prevent the corrosion problem, micro-destructive analyses have been carried out on the polished lower face of each studied tesserae (see, Zacarias *et al.*, 2020).

These findings suggest – in agreement with Lahilil (2011) – that in all the studied samples the $Pb_2Sb_2O_7$ phase synthesized ex-situ was added to the molten glass, and homogenized by mechanical techniques (stirring). This hypothesis is also confirmed by a number of studies (Shortland, 2002; Sabatino *et al.*, 2003;

2007; Spadaro et al., 2007), that synthesized the bindheimite following the recipe reported by Piccolpasso (1548). In particular, they mixed in a mortar, basic lead carbonate ($2\text{PbCO}_3(\text{OH})_2$), stibnite (Sb_2S_3), antimony trioxide (Sb_2O_3), potassium aluminum sulphate ($\text{KAl}(\text{SO}_4)$) and ammonium chloride (NH_4Cl), at temperature of about 550–650 °C, to obtain after 5 hours the bindheimite as main phase (> 75%) plus other minor phases such as rosielite (hexagonal Pb antimonite, PbSb_2O_6), anglesite, antimony oxide and hydroxide. The results of this experiment are in agreement with those carried out by Dick et al. (2007).

5. CONCLUDING REMARKS

The overall results of this study evidenced the presence of both lead stannate and lead antimonate in the analyzed yellow tesserae. According to Lahlil et al. (2011), we confirmed that:

- lead stannate occurred in yellow tesserae from Roman mosaics ranging in age from the 2nd BC to the 5th AD century.

AUTHOR CONTRIBUTIONS

Conceptualization, M.D.B., G.S., M.A.M. and M.T.; methodology, G.S. and M.T.; formal analysis, G.S., G.M. and A.F.M.; investigation, M.D.B. and G.S.; resources, M.T., G.S., M.A.M. and A.T.; data curation, G.S., G.M. and A.F.M.; writing – original draft preparation, M.D.B.; writing – review and editing, M.A.M., F.I., M.T. and A.T.; supervision, M.D.B., G.S. and M.A.M.; project administration, M.D.B., G.S. and A.T.; funding acquisition, A.T. All authors have read and agreed to the published version of the manuscript.

ACKNOWLEDGEMENTS

We would like to thank the Soprintendenza ai Beni Culturali of Enna to kindly provide samples of tesserae from mosaics of “Villa del Casale” archeological site. The Museo Regionale of Messina and the Museo Antiquarium “Badia” of Tusa (ME) are thanked for the mosaic tesserae of Lipari and Tusa respectively.

REFERENCES

- Arletti, R. (2005) The ancient Roman glass: an archaeometrical investigation. PhD thesis, Università di Modena e Reggio Emilia
- Arletti, R., Giordani, N., Tarpini, R. and Vezzalini, G. (2005) Archaeometrical analysis of glass of western Emilia Romagna (Italy) from the Imperial Age, *Annales du 16 e Congrès de l'Association Internationale pour l'Histoire du Verre*, London 2003, Nottingham pp. 80-84.
- Arletti, R., Quartieri, S., Sabatino, G., Triscari, M., Vezzalini, G., Ciarallo, A., Mastelloni, M. A. (2005) Il vetro opaco in epoca romana: studio di pedine e di tessere vitree da Pompei e siti siciliani. *Atti Congr AIAR 2005*, Caserta.
- Arletti, R., Ciarallo, A., Quartieri, S., Sabatino, G., Vezzalini, G. (2006a) Archaeometric analyses of game counters from Pompeii. In: Maggetti M, Messiga B (eds) *Geomaterials in Cultural Heritage*. (257:175–186). *Geological Society, London, Special Publications*.
- Arletti, R., Quartieri, S., Vezzalini, G. (2006b) Glass mosaic tesserae from Pompeii: an archaeometrical investigation. *Per Mineral*, Vol. 76, pp. 25–38.
- Arletti, R., Giacobbe, C., Quartieri, S., Sabatino, G., Tigano, G., Triscari, M., Vezzalini, G. (2010) Archaeometrical investigation of Sicilian early. Byzantine glass: chemical and spectroscopic data. *Archaeometry* 52:99–114.
- Arletti, R., Vezzalini, G., Fiori, C., Vandini, M. (2011) Mosaic glass from St. Peter's, Rome: manufacturing techniques and raw materials employed in late 16th-century Italian opaque glass. *Archaeometry*, 53:364–386
- Augusti, S. I (1967) *Colori Pompeiani*; De Luca Editore—Ministerio della Pubblica Istruzioni, Direzioni Generale delle Antichità e Belle Arti: Rome, Italy, 1967

- yellow crystals were synthesized before being added to glass;
- process at different scales has been used to produce lead antimonate as evidenced by values of Pb/Sb ratio and heterogeneities in the crystal aggregates, indicating that no strict recipe was utilized;
- a Sb, Sn and Fe-rich raw material was used to produce antimonate compounds, it is different from that Zn and Fe rich used to produce Egyptian glass.

We can conclude that lead stannate is present in ancient yellow glass dated before 4th century. The problem of the origin of Sn remains undefined, since from a geochemical point of view it is incompatible with a natural source of Sb and Pb. Therefore, we think that further research in this regard could be important to learn more about glassmaking techniques throughout history.

- Belfiore, C. M., Mazzoleni, P., Manenti, A. M., Mastelloni, M. A., Corsale, V., Barone, G. (2021) Non-destructive XRF analysis of Aegyptiaca from Sicilian archaeological sites. *Mediterranean Archaeology and Archaeometry*, 21(1):37-69. DOI: 10.5281/zenodo.4284407
- Biringuccio, V., (1540) De la Pirotechnia, (eds. Mieli A.), Società tipografica editrice barese, Bari, 1914.
- Bimson, M. and Werner, A. E. (1969) Two problems in ancient glass opacifiers and Egyptian core materials, in *Annales du 4° Congrès International d'Étude Historique du Verre*, 13–20 Mai 1967, Ravenne–Venise (ed. J. Philippe), 262–6, *Journales Internationales du Verre*, Liège.
- Boeselager, D. V. (1989) Funde und Darstellungen Römischer Schreibzeugfalter zur Deutung einer Beigabe in Kölner Gräbern. *Kölner Jahrbuch für vor- und Frühgeschichte*, 22:221-239
- Cascales, C., Rasines, I., Garcia Casado, P., Vega, J. (1985) The new pyrochlores $Pb_2(M_{0.5}Sb_{1.5})O_{6.5}$ (M = Al, Sc, Cr, Fe, Ga, Rh), *Materials Research Bulletin*, 20:1359–1365.
- Cascales, C., Alonso, J.A. and Rasines, I. (1986) The new pyrochlores $Pb_2(MSb)O_{6.5}$ (M=Ti, Zr, Sn, Hf)', *Journal of Materials Science Letters*, 5:675-677.
- Charlesworth, M. P. (1924) Trade Routes and Commerce of the Roman Empire, (Georg Alms Press, London, 1924) Cambridge: Cambridge University Press, 1926 xxiii, 296 p., maps.
- Clayton, R. E., Scrivener, R. C., Stanley, C. J. (1990) Mineralogical and preliminary fluid inclusion studies of lead-antimony mineralisation in north Cornwall. *Proceedings of the Ussher Society* 7:258–262.
- Croveri P., Fragalà I., Ciliberto E. (2010) Analysis of glass tesserae from the mosaics of the 'Villa del Casale' near Piazza Armerina (Enna, Italy). Chemical composition, state of preservation and production technology. *Appl Phys A Mater Sci Process* 100:927–935
- Dana, J. D. and Dana, E. S. (1951) The System of Mineralogy. (Wiley and Sons, New York, 1951). 2:1018–1019.
- De Francesco, A. M., Scarpelli, R., Conte, M. and Toniolo, L. (2019) Characterization of Roman glass from Casa Bacco deposit at Pompeii by wavelength-dispersive electron probe microanalysis (EPMA). *Mediterranean Archaeology and Archaeometry*, 19(3):79-91. DOI: 10.5281/zenodo.3541106
- Dessau, G. (1951) Geologia e depositi di antimonio e d'altri metalli del Gruppo dei Monti Romani (Comune di Manciano, Maremma Toscana). *Boll. Soc. Geol. d'It.* v. LXX, fas. I, Mancianese.
- Di Bella, M., Sabatino, G., Giuliano, A., Italiano, F., Quartieri, S., Triscari, M., Magazù, S., Tripodo, A. (2020) New spectroscopic data on "marmi mischi" Baroque glass decorations from "Palliumaltaris" of Messina (Sicily, Italy). *Mediterranean Archaeology and Archaeometry*, 20(2):97-111. DOI: 10.5281/zenodo.3819595
- Dik, J., Hermens, E., Peschar, R., and Schenk, H. (2005) Early production recipes for lead antimonate yellow in Italian art, *Archaeometry*, 47, 593–607.
- Donovan, J., Rivers, M.L. (1990) PRSUPR-A PC based automation and analyses software package for wavelength-dispersive electron beam microanalysis. In: Michael JR, Ingram P (eds) *Proc. Micro-Beam Analysis Society*, San Francisco, p. 66
- Freestone, I.C., Ponting, M., Hughes, M.J. (2002a) The origins of Byzantine glass from Maroni Petrera, Cyprus. *Archaeometry*, Vol. 44, pp. 257–272.
- Freestone, I.C., Greenwood, R., Gorin, R.Y. (2002b) Byzantine and Early Islamic glassmaking in the Eastern Mediterranean: production and distribution of primary glass. In: *1st International Conference: Hyalos, vitrum, glass; history, technology and conservation of glass and vitreous materials in the Hellenic world*. Athens, pp. 167–174
- Galli, S., Mastelloni, M.A., Ponterio, R., Sabatino, G., Triscari, M. (2004) Raman and scanning electron microscopy and energy-dispersive X-ray techniques for the characterization of coloring and opaquening agents in Roman mosaic glass tesserae. *J Raman Spectrosc*, 35:622–627M.
- Gelzo, M., Corso, G., Vergara, A., Rossi, M., Miedico, O., Arcari, O., Chiaravalle, A. E., Piccioli, C., Arcari, P. (2021) Archaeometric studies on a blue glass fragment from Pompeii: case study. *Mediterranean Archaeology and Archaeometry*, 21(3):23-34. DOI: 10.5281/zenodo.5545711
- Gentili, G.V. (1954) La Villa Imperiale di Piazza Armerina. *Ed. Istituto poligrafico dello Stato*, Libreria dello Stato, pp. 1–91.
- Giustetto, R., Gonella, D. and Diana, E. (2018) decay of red pigments on a wall painting adorning the church of 'San Francesco dei Capuccini' in Racconigi (Italy): archaeometric survey and restoration intervention. *Mediterranean Archaeology and Archaeometry*, 18(5):65-80. DOI: 10.5281/zenodo.1256055
- Hedges, R. E. M. (1976) Pre-Islamic Glazes in Mesopotamia-Nippur, in: *Archeometry*, 18(2):209-213.
- Henderson, J. (1985) The raw materials of early glass production. *OJA* Vol. 4, pp. 267–291.

- Hradil, D., Grygar, T., Hradilova, J., Bezdicka, P., Grünwaldova Fogas, I. and Miliani, C. (2007) Microanalytical identification of Pb–Sb–Sn yellow pigment in historical European paintings and its differentiation from lead tin and Naples Yellows, *Journal of Cultural Heritage*, 8(4), 377–86.
- Kaplan, Z., Ipekoglu, B., and Boke, H (2017) physicochemical properties of glass tesserae in roman terrace house from ancient antandros (base glass, opacifiers and colorants). *Mediterranean Archaeology and Archaeometry*, 17(1):141-157. DOI: 10.5281/zenodo.258103
- Kirmizi, B., Göktürk, E. H. and Colombari, P.H. (2014) Colouring agents in the pottery glazes of Western Anatolia: new evidence for the use of Naples Yellow pigment variations during the Late Byzantine Period, *Archaeometry*, doi: 10.1111/arc.12101
- Lahil, S., Biron, I., Cotte, M., Susini, J. (2010) New insight on the situ crystallization of calcium antimonate opacified glass during the Roman period, *Appl Phys A* 100:683–692
- Lahil, S., Cotte, M., Biron, I., Szlachetko, J., Menguy, N., Susini, J. (2011) Synthesizing lead antimonate in ancient and modern opaque glass, *J Anal At Spectrom* 26:1040–1050
- Lilyquist, C., Brill, R.H. (1995) Studies in ancient Egyptian glass, *Metropolitan Museum of Art*. New York.
- Mass, J.L., Wypyski, M.T., Stone, R.E. (2002), Malkata and Lisht glassmaking technologies: toward a specific link between second millennium BC metallurgist and glassmaker, *Archaeometry*, 44:67-82.
- Mass, J. L., Stone, R. E. and Wypyski, M. T. (1997) Materials Research Society Symposium Proceedings, 462, p. 193.
- Mass, J. L., Stone, R. E., and Wypyski, M. T. (1998) The mineralogical and metallurgical origins of Roman opaque colored glasses, in The prehistory and history of glassmaking technology (eds. P. McCray and W. D. Kingery), 121–44, *Ceramics and Civilization*, vol. 8, *The American Ceramics Society*, Westerville, OH.
- Mastelloni, M.A. (2001) Tusa (Me): pavimenti da uno scavo di A. Salinas (1912). Nota preliminare, in AISCOM VIII, 2001, pp. 689-704
- Mastelloni, M.A. (2004) Tessere vitree da pavimenti musivi della Sicilia Nord Orientale e di Lipari, in Glassway. Il vetro: fragilità attraverso il tempo Catalogo Mostra Castello di Donnafugata, Ragusa 26 giugno - 31 luglio, Ragusa, pp.123-128
- Mastelloni, M.A. (2005) Pavimenti e mosaici di Messina, in Lo Stretto di Messina nell'antichità, a cura di F. Ghedini, J. Bonetto, A.F. Ghiotto, F. Rinaldi, Roma 2005, 485-500.
- Mastelloni, M. A., Triscari, M., Sabatino, G. (2011) Il mosaico da Lipari (Me) con Europa su toro e le quattro stagioni ed alcuni frammenti di Tusa (Me), Loc. Lancinè: analisi formali ed esami sperimentali, in XVI CollAssIt a Studio Conservazione Mosaico, Palermo 17 - 20 /03/10, Tivoli 2011, pp. 37-48.
- Piccolpasso, C. (1548) Li tre libri dell'arte del vasajo, eds. All'Insegna del Giglio, 2006.
- Raneri, S., Cantini, F., Belcari, R., Baldanza, A., Bertinelli, A., Lorenzetti, G., Legnaioli, S., Mazzoleni, P., Lezzerini, M. (2018) Building materials and architectural models in late Roman Tuscany. archaeometric studies on mortars, stones and vitreoustesserae from "Villa dell'oratorio" (Florence). *Mediterranean Archaeology and Archaeometry*, 18(5):109-129. DOI: 10.5281/zenodo.1285889
- Rosi, F., Manuali, V., Miliani, C., Brunetti, B. G., Sgamellotti, A., Grugar, T. and Hradil, D., (2009) Raman scattering features of lead pyroantimonate compounds. Part I: XRD and Raman characterization of Pb₂Sb₂O₇ doped with tin and zinc, *Journal of Raman Spectroscopy*, 42, 407–14
- Sabatino, G., Quartieri, S., Triscari, M. (2003) Origine e significato tecnologico dell'antimoniato di piombo nel giallo di paste vitree di età romana. I° Giornata scientifica del Gruppo Naz. Georisorse, Ambiente e Beni Culturali, Dip. Scienze della Terra, Univ. Napoli, 5/12/2003, 9.
- Sabatino, G. (2007) Vetri archeologici di età romana (dal II sec. a.C. al VI sec. d.C.) in Sicilia: attribuzione di provenienza e caratterizzazione delle tecniche costruttive. PhD thesis, Università di Messina
- Sayre, E.V., Smith, R.W. (1974) Analytical studies of ancient Egyptian glass. In: Recent advanced in science and technology of materials, Cairo. Solid state conference, 2. Plenum, New York, pp. 40–70
- Seccaroni, C. (2006) Giallorino: storia dei pigmenti gialli di natura sintetica, De Luca, Roma.
- Shortland, A.J. (2002) The use and origin of antimonate colorants in Early Egyptian Glass. *Archaeometry*, Vol. 44, pp. 517–531.
- Shortland, A.J. (2005) The raw materials of early glasses: the implications of new LA-ICP-MS analyses. In: Cool H (ed.) Proceedings of the 16th International Congress of the Association Internationale pour l'Histoire du Verre, London, 2003, pp. 1–5.
- Shortland, A.J., Eremin, K. (2006) The analysis of second millennium glass from Egypt and Mesopotamia, part 1: new WDS analyses, *Archaeometry*, Vol. 48, pp. 581–603.

- Spadaro, D., Sabatino, G., Triscari, M. (2007) L'antimoniato di piombo: approccio sperimentale per la realizzazione di tessere musive. Dissertation. A.I.Ar., "Colore ed arte: storia e tecnologia del colore nei secoli", Firenze
- Tanevska, V., Colombari, P.H., Minceva-Šukarova, B. and Grupc̆e, O. (2009) Characterization of pottery from the Republic of Macedonia I: Raman analyses of Byzantine glazed pottery excavated from Prilep and Skopje (12th–14th century), *Journal of Raman Spectroscopy*, 40, 1240–8.
- Tite, M., Pradell, T., Shortland, A. (2008) Discovery, production and use of tin-based opacifiers in glasses, enamels and glazes from the Late Iron Age onwards: a reassessment. *Archaeometry* 50(1):67–84
- Triscari, M., Quartieri, S., Sabatino, G., Vezzalini, G., Mastelloni, M. A., Santalucia, F. (2007) Caratterizzazione chimica e spettroscopica di tessere musive in pasta vitrea da siti archeologici siciliani. Atti del Workshop "Tecniche di analisi non distruttive di materiali lapidei naturali e artificiali nei Beni Culturali", Palermo, 22/2/2007, pp. 110–114
- Turner WES (1956) Studies in ancient glasses and glassmaking processes. Part IV: the chemical composition of ancient glasses, *J Soc Glass Technol*, Vol. 40, pp. 162–186.
- Turner, W. E. S. and Rooksby, H. P. (1959) A Study of Opalising Agents in Ancient Opal Glasses throughout Three Thousand Four Hundred Years, in: *Glastechnische Berichte*, Heft 8, 1959, p. 17–28.
- Verità, M. (1995) Le analisi dei vetri. In: Foy D (ed) 'Le Verre de l'Antiquité Tardive et du Haut Moyen Age'. Musée Archeologique Departemental du Val d'Oise, 291–300.
- Wainwright, I. N. M. R., Taylor, J. M. and Harley R. D. (1986) Lead antimonate yellow, in *Artists' pigments: a handbook of their history and characteristics* (ed. R. L. Feller), vol. 1, 219–54, Cambridge University Press, Cambridge, UK/National Gallery of Art, Washington, DC.
- Wilson, R. J. A. (1982) "Roman Mosaics in Sicily: The African Connection." *American Journal of Archaeology*, 86(3):413–428.
- Zacharias, N., Palamara, E., Kordali, T., and Muros, V (2020) Archaeological glass corrosion studies: composition, environment and content. *SCIENTIFIC CULTURE*, Vol. 6, No. 3, pp. 53–67. DOI: 10.5281/zenodo.4007562